Some Two-Point Statistical Properties of a Three-Dimensional Wall Jet

J. B. Morton,* G. D. Catalano,† and R. R. Humphris‡
University of Virginia, Charlottesville, Va.

The effects of both a straight and a curved wall on the two-point space-time velocity correlations of a turbulent jet are documented. From the correlations, isocorrelation contours are constructed which allow a picture of the various flow patterns to be determined. Auto-and cross-correlations of the fluctuating concentration field are also obtained for the different flow configurations. The confining surfaces served to radically change the flow pattern for the freely expanding turbulent jet. The velocity measurements are made with a laser Doppler velocimeter in conjunction with a phase locked-loop processor, while the concentration field is monitored with a laser light-scattering technique.

I. Introduction

TWO previous reports[1,2] have dealt with an experimental investigation of a coflowing axisymmetric jet. In the first study, detailed mappings of one-point statistical properties, such as mean velocities, turbulent intensities, and intermittencies, were made between zero and eight diameters downstream from the jet exit plane. Autocorrelation and power spectral density curves were obtained for both the fluctuating velocity and concentration fields. One of the most significant results noted was the appearance of a peak in the velocity spectra in the potential core region of the flow which reinforces the vortex street model of the turbulent jet.[3,4]

The second study sought to determine the effect of wall surfaces with different radii of curvature on the flowfield of the axisymmetric jet. Of primary concern was the comparison of one-point statistical properties measured at the same position in the flowfield relative to the exit plane of the jet, with and without the wall structures present. The curved wall surface served to break up the potential core region of the jet much more quickly than was the case for either the unconfined flow or the flow over the flat wall. Measurement of the mean velocity in the vertical direction for the flow over the curved wall seemed to indicate that the jet was revolving or rolling up as it spread out over the surface.

The purpose of this investigation is to continue with the comparison of the one- and two-point statistical properties of the unconfined jet, the jet flowing over a flat wall, and the jet flowing over a curved surface. Emphasis is placed on obtaining space-time correlations in the different turbulent flowfields and then constructing an isocorrelation contour map. The work presented in this report will add to the present understanding of large-scale structures in turbulent jets and the effects of confining surface on the flowfield. One direct practical application is to the upper surface blowing (USB) concept being considered as a possible V/STOL technique.

In recent years, investigators have focused much attention on searching for the existence of large-scale structures in turbulent flowfields. Kline and Runstaler[5] and Brown and Roshko[6] reported observations that have had a significant effect on the direction of subsequent turbulent research. They reported that in turbulent flows of simple geometry there is some order in the motion with an observable chain of events reoccurring randomly with a statistical definable mean.

One of the simplest flow geometries is that of a circular turbulent jet. Davies[7] described the main physical features of a subsonic turbulent jet. Crow and Champagne[8] studied the evolution of orderly flow with increasing Reynolds number in their investigation of the noise-producing region of a jet. An investigation of coherent motions in the first ten diameters of round jets was described by Yule.[9] The turbulent flow was dominated by the interacting and coalescing of ring vortices. The large organized structures in the turbulent region of the flowing fluid differ fundamentally from the laminar ring vortices at the exit plane. These structures possessed a strong and well-ordered three-dimensional nature. Favre[10] also pioneered work in this area with his velocity measurements downstream of a grid in a boundary layer. The measurements were of the space-time double correlations, i.e., double velocity correlations with both spatial separation and time delay, from which isocorrelation lines for optimum delay can be determined. According to Favre,[11] the space-time correlation can give evidence of the heredity of turbulence, as well as the convection velocities of the vorticity and entropy bearing modes as compared to the average mass-transport velocities. It also allows the separation of the acoustical mode, the propagation velocity of which is known, and thus the determination of the position and the convection velocity of sources of aerodynamic noise. Sternburg[12] sought to interpret space-time correlation measurements in a shear flow. In shear flows, the inapplicability of Taylor's hypothesis has been recognized and examined by several authors.[13,14] Specifically, Sternburg considered the effect of the mean shear on the turbulence, and directed his thoughts toward a simple explanation for the shapes of the curves of maximum correlation, as reported by Favre.[11]

II. Experimental Equipment and Techniques

The flow system consists of a jet whose compressed air is marked with diocytl phthalate (DOP) mounted inside the test section of a low-turbulence-level subsonic wind tunnel. With the parallel secondary flow in the wind tunnel being kept at a constant speed of 3.20 m/s, the ratio of the exit plane velocity of the jet (16.30 m/s) to velocity of the tunnel flow λ_j is 5.1:1. The jet nozzle has a contraction ratio of 14:1 over a length of 15.9 cm. The Reynolds number of the jet flow is 22,600, using the nozzle diameter (2.14 cm) as the length scale. The test section of the wind tunnel is 23×30.5 cm.

Received Oct. 13, 1977; revision received March 16, 1978.

Index category: Jets, Wakes, and Viscid-Inviscid Flow Interactions.
*Associate Professor, Dept. of Mechanical and Aerospace Engineering. Member AIAA.
†Current address: AFFDL/FXM, Wright Patterson Air Force Base, Ohio.
‡Senior Scientist, Department of Nuclear Engineering and Engineering Physics.

At the exit plane of the nozzle, the velocity is zero over the thickness of the lip. The wake caused by the presence of the nozzle in the wind tunnel extends approximately one diameter laterally from the centerline of the contraction section. At this lateral location, the velocity in the tunnel has reached its freestream value. This region of slower moving air is essentially eliminated six diameters downstream from the exit plane. It should also be pointed out that for all downstream locations at which measurements are made, the width of the jet's flowfield is significantly smaller than either the width of the flap or plate or that of the test section.

Davies[7] has found that the behavior of the large-scale structure in the near-field region of various turbulent jets is similar, provided the Reynolds number of the flow is greater than approximately 10,000.

The curved wall surface, henceforth denoted "flap," is a 1/12th scale model of an actual airfoil surface being used in a USB investigation at NASA Langley.[15] Thus, the particular value of the velocity ratio parameter, $\lambda_j = 5.1$, is chosen because that value is representative of a possible flowfield condition for this type (USB) of V/STOL aircraft during take-off and landing. In a forthcoming report, some of the effects of varying the value of the velocity ratio parameter will be discussed. The flap is composed of a flat surface 17.80-cm wide and 7.50-cm long and a curved portion with a radius of curvature of 6.50-cm and sweeping out an arc of 70 deg. The flat wall surface, henceforth denoted "plate," is 30.50-cm wide and 30.50-cm long. The leading edges of the plate and flap were contoured to provide as small a disturbance as possible to the tunnel flow.

In Fig. 1, schematics of the jet/flap and jet/plate configuration as well as the coordinate system used are shown. Care was exercised to insure a smooth transition between the inner surface of the nozzle and the upper surface of the walls.

The velocity measurements are made by a laser Doppler velocimeter (LDV) in conjunction with a phase locked-loop processer. In order to measure the velocity fluctuations at two separate points in the flowfield, a two-color LDV setup is designed. An argon ion laser is used in the all-lines mode of operation with the strongest two frequencies of light selected for use. The basic components of the simpler one-point LDV system are shown in Fig. 2. To make the concentration and

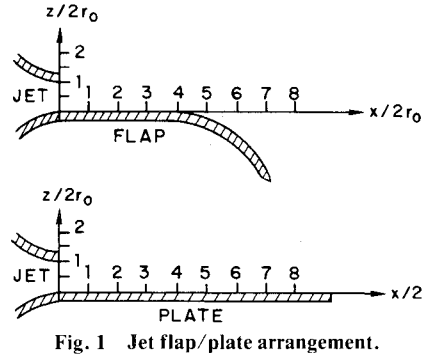

Fig. 1 Jet flap/plate arrangement.

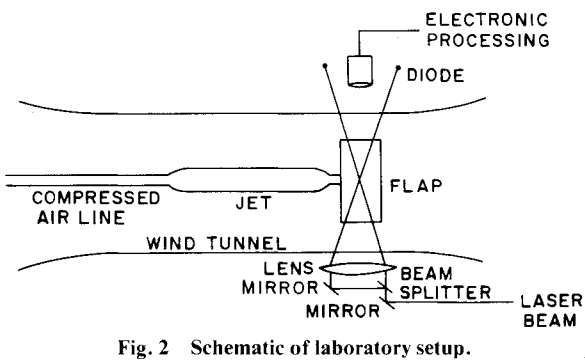

Fig. 2 Schematic of laboratory setup.

intermittency measurements, a laser light-scattering technique developed by Shaughnessy and Morton[16] is employed.

In the use of an LDV for measurements in a highly intermittent turbulent flow, signal dropout is often a problem. An experimental test to examine the behavior of the phase locked-loop processor when Doppler signals are not present has been documented previously,[1] the main conclusion(s) being that meaningful mean and fluctuating velocity measurements can be made even in highly intermittent regions.

III. Experimental Results

Concentration Auto- and Cross-Correlations

The concentration auto- and cross-correlations are defined in a similar manner as those determined for the velocity field. However, it is the fluctuations of the passive admixture (DOP) that are being monitored rather than the turbulent velocity fluctuations. The autocorrelation function of the concentration field is defined as

$$R_c = \overline{cc^*}/[(\overline{c^2})^{1/2}(\overline{c^{*2}})^{1/2}]$$

where

$$c = c(x,y,z,t) \quad \text{and} \quad c^* = c(x,y,z,t+\Delta t)$$

Consider the cross-correlation function of the concentration field, defined in the restricted manner such that only lateral or y displacements are allowed between the two measuring points. Then the cross-correlation takes the following form:

$$Rc_1c_2 = \frac{\overline{c_1(x,y,z,t)\,c_2(x,y+\Delta y,z,t+t)}}{(\overline{c_1^2})^{1/2}(\overline{c_2^2})^{1/2}}$$

where c_1 and c_2 are the concentration fluctuations at two different points in the flowfield.

Next, the further restriction is made that the concentration fluctuations will be monitored only at the lateral positions corresponding to the lip of nozzle ($y/2r_0 = \pm 0.5$) at the vertical location $z/2r_0 = 0.5$.

Recall the vortex street model of a turbulent jet. The model theorizes that vortices are shed from the lip of the nozzle and move downstream. The frequency of the passing of the vortices through a particular downstream location in the flowfield will show up in the correlation function as a sinusoidally shaped curve. The time between the peaks corresponds to the dominant frequency of the flow. As the turbulence level increases or the separation (space or time) between the measuring points increases, the sinusoidally shaped curve will become more damped.

Auto- and cross-correlations are measured in the three flow configurations at different downstream locations. Consider initially the case of the unconfined coflowing jet. Data are presented for $x/2r_0 = 4$ and 8 in Figs. 3 and 4, respectively. At $x/2r_0 = 4$, the autocorrelation of the concentration fluctuation is quite similar to the velocity autocorrelation functions discussed earlier in a previous report.[2] The curve demonstrates a damped sinusoidal behavior. The cross-correlation curve, measured with one sampling volume on each side of the jet, is also of a similar shape. The maximum absolute value of the coefficient ($Rc_1c_2 = 0.12$) occurs at approximately zero-delay time, though there is evidence of a slight phase shift between the two concentration signals. A phase shift in the cross-correlation indicates that there a temporal delay in the relationship between the fluctuations in the concentration field at opposite lateral locations downstream from the nozzle. An increase in the phase shift implies an increase in the temporal lag. At $x/2r_0 = 8$, the autocorrelation curve is of a more typically fully turbulent nature. The maximum ab-

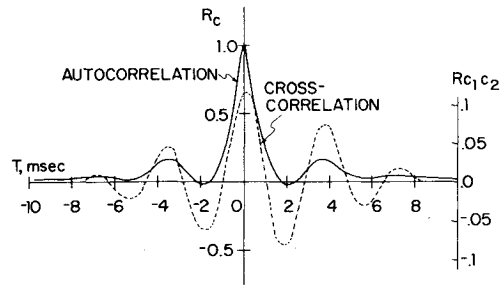

Fig. 3 Auto- and cross-correlations for jet concentration field, $x/2r_0 = 4$, $y/2r_0 = \pm 0.5$, $z/2r_0 = 0.5$ ($\lambda_j = 5.1$).

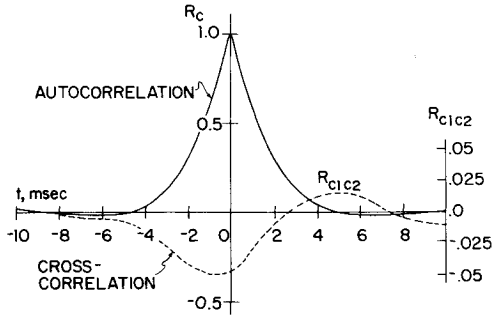

Fig. 4 Auto- and cross-correlations for jet concentration field, $x/2r_0 = 8$, $y/2r_0 = \pm 0.5$, $z/2r_0 = 0.5$ ($\lambda_j = 5.1$).

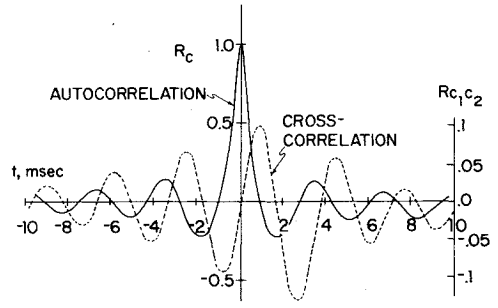

Fig. 5 Auto- and cross-correlations for jet/plate concentration field, $x/2r_0 = 4$, $y/2r_0 = \pm 0.5$, $z/2r_0 = 0.5$ ($\lambda_j = 5.1$).

solute value of the cross-correlation coefficient has significantly decreased ($Rc_1c_2 = 0.05$), though there still is some relation between the fluctuating concentration field at $y = \pm 0.5$. A large shift in the phase angle between the signals has also occurred.

Auto and cross correlations for the flow over the plate are presented in Figs. 5 and 6 for the downstream positions $x/2r_0 = 4$ and 8. The autocorrelation coefficient curve at $x/2r_0 = 4$ is quite similar to that found for the case of the unconfined jet at $x/2r_0 = 4$. The maximum absolute value of the cross-correlation coefficient is similar to the previous case as well ($Rc_1c_2 = 0.13$). The delay time for the maximum coefficient value has been shifted in the positive time direction. The concentration signals are considerably more out of phase than is the case for the unconfined jet. At $x/2r_0 = 8$, the damped sinusoidal nature of the autocorrelation coefficient curve has disappeared. The maximum absolute value of the coefficient has decreased ($Rc_1c_2 = 0.04$). As in the case of the unconfined jet, though the concentration autocorrelation curves appear to be fully turbulent in nature, there still is evidence of a relationship (albeit a weak one) between the fluctuations at the lip of the nozzle.

Finally, consider the flow of the jet over the flap. Auto- and cross-correlations at $x/2r_0 = 4$ are presented in Fig. 7. The autocorrelation coefficient is quite similar in shape to the

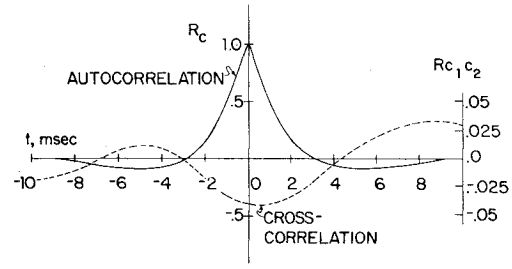

Fig. 6 Auto- and cross-correlations for jet/plate concentration field, $z/2r_0 = 8$, $y/2r_0 = \pm 0.5$, $z/2r_0 = 0.5$ ($\lambda_j = 5.1$).

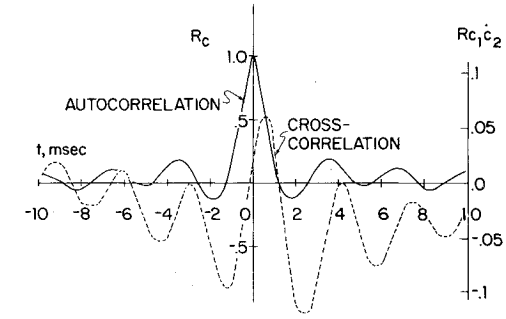

Fig. 7 Auto- and cross-correlations for jet/flap concentration field, $x/2r_0 = 4$, $y/2r_0 = \pm 0.5$, $z/2r_0 = 0.5$ ($\lambda_j = 5.1$).

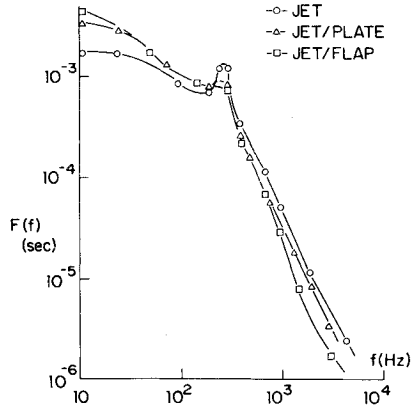

Fig. 8 Concentration spectra comparison, $x/2r_0 = 4$, $|y|/2r_0 = 0.5$, $z/2r_0 = 0.5$ ($\lambda_j = 5.1$).

previous two cases for this downstream location. The maximum absolute value of the cross-correlation coefficient is also comparable ($Rc_1c_2 = 0.12$). The cross-correlation coefficient curve, much like the case for the flow over the plate, demonstrates a large phase shift between the concentration fluctuations at $y/2r_0 = \pm 0.5$.

Concentration Field Spectra

A spectrum of concentration or contaminant fluctuations is produced when smoke particles are mixed by the turbulent flowfield of the jet. Many of the same concepts that are used in describing the kinetic energy spectrum can be applied to the spectra of the mixing smoke particles. Velocity spectra for the three flow configurations have been documented in a previous report.[2] The scales of the smoke particle fluctuations range from the scale of the energy-containing eddies to a smallest scale that is dependent on the ratio of the diffusivities (Schmidt number). The spectra are normalized for unit area.

Concentration spectra measured for the three flow configurations are shown in Figs. 8 and 9. In Fig. 8, the laser "probe" is positioned at $x/2r_0 = 4$, $|y|/2r_0 = 0.5$, and $z/2r_0 = 0.5$. Consider first the case of the unconfined

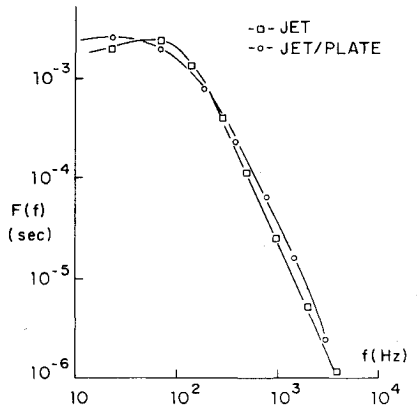

Fig. 9 Concentration spectra comparison, $x/2r_0=8$, $|y|/2r_0=8$, $z/2r_0=0.5$ ($\lambda_j=5.1$).

coflowing jet. Notice the relatively large peak in the spectra at approximately 300 Hz. The peak in the spectra corresponds to the passing downstream of vortices shed at the lip of the nozzle. With the plate placed in the flowfield, the peak is attenuated and there is an increase in the energy at lower frequencies. By replacing the plate with the flap, this same trend is continued. The peak is diminished further and the energy at the lower frequencies is slightly increased.

In Fig. 9, the concentration spectra of the jet and jet/plate flow are presented for the following downstream location: $x/2r_0=8$, $|y|/2r_0=0.5$, and $z/2r_0=0.5$. At eight diameters downstream, the peak in the spectra has disappeared. Here again, the presence of the plate in the flowfield has caused an increase in energy of the concentration spectra at low frequencies.

Space-Time Two-Point Velocity Correlations

The general space-time correlation coefficient for two points separated in a given flowfield is:

$$R_{1,1}(x,y,z,t,\xi_1,\xi_2,\xi_3,\tau) = \frac{\overline{u(x,y,z;t)\,u'(x+\xi_1,y+\xi_2,z+\xi_3;t+\tau)}}{\{\overline{u^2}\}^{1/2}\{\overline{u'^2}\}^{1/2}}$$

where ξ_1,ξ_2, and ξ_3 represent the spatial displacements of one point relative to the other and τ represents the delay time. Here, the space-time correlations are limited in scope to fluctuating velocities in the x direction only. From these measurements, it is possible to calculate isocorrelation curves for optimum delay, τ_m. Optimum delay time refers to the delay time at which the correlation is a maximum.

Typical results obtained are shown in Figs. 10-15. Figures 10-12 deal with the case when ξ_2 is set equal to zero and hence are cross-sectional views of the three flowfields in the x-z plane. Figures 13 and 15 correspond to the isocorrelation curves obtained with ξ_1 set equal to zero, and thus represent cross-sectional views in the y-z plane.

The reference point which remains fixed for all the correlation coefficients determined in the three flows has the following coordinates:

$$x/2r_0=4 \quad y/2r_0=0 \quad z/2r_0=0.5$$

This downstream location is chosen for several reasons. First, this is the position at which the flap first begins to curve in a convex manner from the x direction. Secondly, it has been observed in many of the one-point measurements presented earlier in this report, that there are significant differences in the three flows at this position and, also, the statistical properties have been carefully documented.

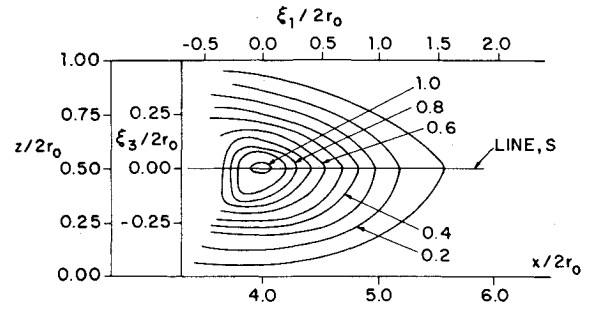

Fig. 10 Isocorrelation curves for jet in x-z plane ($\lambda_j=5.1$).

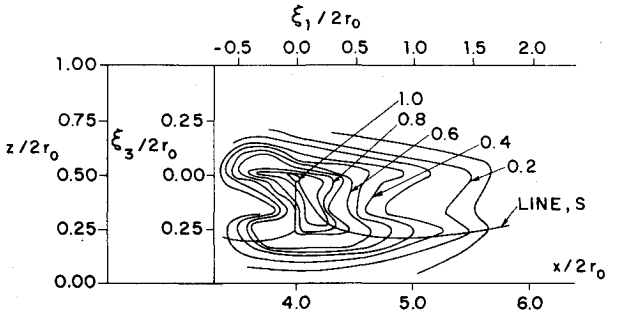

Fig. 11 Isocorrelation curves for jet/plate in x-z plane ($\lambda_j=5.1$).

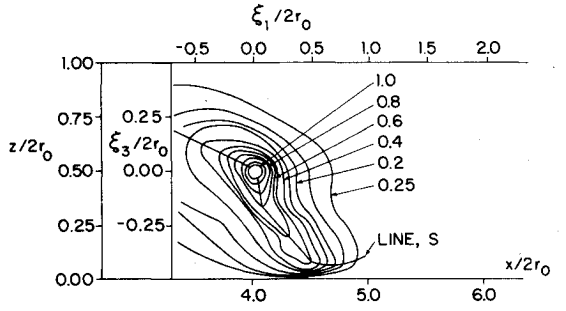

Fig. 12 Isocorrelation curves for jet/flap in x-z plane ($\lambda_j=5.1$).

Before progressing further, a new term must be introduced—the line of maximum maximorum of the correlations. Physically what is meant is that a line S is drawn through the point on each correlation level, which is separated the farthest amount from the reference point, i.e., $(\xi_1^2+\xi_2^2)^{1/2}$ or $(\xi_2^2+\xi_3^2)^{1/2}$ is a maximum. With this line, it is then possible to get an idea of the flow pattern. The pattern of the isocorrelation curves describe, in a qualitative sense, the large-scale structure of the various turbulent flowfields. The line S helps in a comparison to the shapes of the curves. If the turbulent flows can be considered as possessing large eddy structures, the line of maximum maximorum yields information about the sense of the rotation of the eddies and any deformation.

In Fig. 10, the isocorrelation curves in the x-z plane for the case of the unconfined, coflowing jet are shown. The curves are very elongated in the streamwise direction and close to being symmetric with respect to the ξ_1 axis. This is not the case about the ξ_3 axis, which is in contrast with contours presented for a fully developed turbulent boundary layer.[5] Presumably, the difference is due to the fact that part of the flowfield lies in the potential core, while the rest can be considered a mixing region. The line S, marking the points of maximum maximorum of the correlations is approximately straight, which would be the expected behavior.

The isocorrelation curves in the x-z plane for the case of the turbulent jet flowing over the plate are shown in Fig. 11. Once

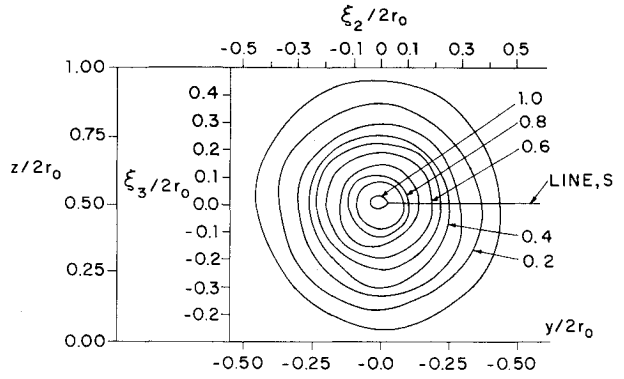

Fig. 13 Isocorrelation curves for jet in y-z plane ($\lambda_j = 5.1$).

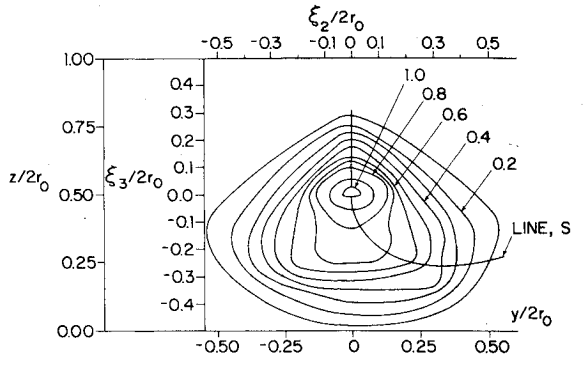

Fig. 14 Isocorrelation curves for jet/plate in y-z plane ($\lambda_j = 5.1$).

again, the curves are elongated in the streamwise direction, and there is no axis of symmetry. The pattern formed by the isocorrelation curves is very complex and is composed partly of two different lobes of high-correlation value levels. The line S is drawn through the points of maximum maximorum of the correlations, as was done in Fig. 10. Downstream of the fixed reference point, the line is convex toward the surface of the wall. Upstream of the reference point, it is slightly more difficult to construct the line, but it also seems to be convex toward the plate's surface. Sternburg[7] has offered a possible explanation of a qualitative nature for the observed shape of the S lines. He theorizes that this may be caused by the mean shear, deforming the turbulence flow pattern as determined by its vorticity distribution. The maximum correlation will be determined by a point of the vorticity pattern that passes the fixed laser control volume at t equal to zero and is observed at some time, τ, later. The larger eddies, which have a longer correlation distance will rotate due to the distortion of the mean shear flow in a clockwise sense and with a center of rotation in x-z plane. As the second movable control volume approaches the plate, a point of the flow pattern passing the fixed laser "probe" at $\tau = 0$ will be displaced on the average from the wall by this rotation for $\tau > 0$, while for $\tau < 0$ this point has arrived from an upstream position also at a greater distance from the wall. The rough picture would lead to an S-line convex toward the wall below the center of rotation, a fairly straight line near the center, and curved concave to the wall above the center.

The isocorrelation contours in the x-z plane for the flow of the turbulent jet over the flap are presented in Fig. 12. As is the case for the plate configuration, the pattern formed by the isocontours is not symmetric about either the ξ_1 or ξ_3 axis. It has been observed before that the previous two contours demonstrated an elongation in the streamwise direction. For the flow over the flap, the elongation exists, but the pattern formed is rotated a sizable amount from the longitudinal direction. The line S is drawn through the points of maximum maximorum of the correlations. Before applying Sternburg's approach, it is first necessary to recall the geometry of the flap and the relative position of the reference "probe." In Fig. 1, a view of the jet/flap assembly is shown. After a distance of approximately four diameters downstream from the exit plane of the nozzle, the tangent to surface of the flap quickly rotates away from the horizontal direction. Thus, any position for the second probe downstream of the $x/2r_0 = 4$ plane would be over the curved section of the flap's surface. Now, consider the shape of the line S in Fig. 12. Downstream of the reference point, the line heads down toward the wall surface and is also convex relative to the flap. Upstream, the line is also inclined with a negative slope from the x direction and is essentially straight. Clearly, it is possible to say from observing the isocorrelation contours that the flow is being turned by the flap. Secondly, considering the change in shape of the flap surface and the convex shape of the line S downstream, Sternburg's ideas can be reasonably applied once again. For the clockwise rotation of the large eddies, a point of the flow pattern passing the reference control volume will tend to both be turned downward by the flap's surface and also be displaced on the average from the wall by this rotation for a positive delay time. The flow pattern upstream of the fixed reference point indicates the direction from which the flow is coming.

In Fig. 13, the isocorrelation curves in the y-z plane for the unconfined coflowing turbulent jet flowfield are shown. The eccentricity of each of the curves does vary, but is essentially zero, and thus the isocorrelation levels are close to being circles in shape. Hence, symmetry in the flow exists about the ξ_2 and ξ_3 axes. Though Sternburg's ideas cannot be applied in the y-z plane, the line S can be constructed, and from its shape a rough estimate of the flow pattern can be obtained. For the unconfined jet, the line of maximum maximorum can be drawn, starting from the center of the field off in any radial direction. One line is arbitrarily constructed for the sake of clarity. From observing the line S and the isocorrelation curves, an indication that the jet's flowfield is spreading out equally in all directions is apparent. The lower correlation levels farther out from the centerline represent fluid particles which have been separated from the potential core the longest period of time.

Consider next the isocorrelation curves in the y-z plane for the flow of the turbulent jet over the plate (Fig. 14). The change in the shape of the curves caused by the presence of the plate is apparent. The isocorrelation curves are elongated in the lateral direction. Although the flow pattern is clearly not symmetric about the ξ_2 axis, symmetry does exist with respect to the ξ_3 axis. As was the case in the x-z plane, the line S is again somewhat more difficult to construct. Allowing some author's discretion, the line S moves out from the center of the flow in a slightly convex manner with respect to the plate's surface. Two impressions can be drawn. First, the turbulent jet is drawn downward toward the plate. Second, there exists an indication that the flow may be rolling up in the outer regions, or at least some type of canted rotating motion of the larger eddies to the longitudinal downstream is being observed. It is instructive to compare the differing flow patterns displayed in Figs. 13 and 14. The width of area enclosed by the isolation curves is significantly smaller for the flow over the plate for $\xi_3 > 0$, about the same for $\xi_3 = 0$, and somewhat larger for the $\xi_3 < 0$. The second observation is reinforced by the measurements made of the mixing widths and the intermittency profiles for the two flows.

Finally, the isocorrelation curves in the y-z plane for the flow of the turbulent jet over the flap are shown in Fig. 15. The isocorrelation curves are markedly elongated in the z direction. The flow pattern is symmetric about the ξ_3 axis, but asymmetric with respect to the ξ_2 axis. The line S is drawn appropriately through the flowfield pattern. The first impression is one of noticing the narrowness of the flow pattern. As has been mentioned previously, the flap is much more

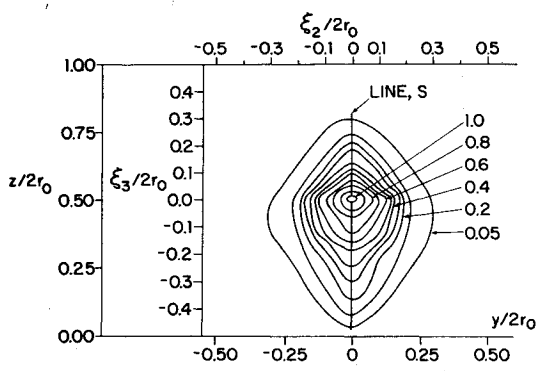

Fig. 15 Isocorrelation curves for jet/flap in y-z plane ($\lambda_j = 5.1$).

effective in amplifying the turbulence levels of the turbulent jet. This more rapid and intense mixing action would manifest itself in a decrease in the coherence of the flowfield pattern. Thus, in the outer mixing region, the turbulent jet is more apt to have forgotten its previous flow conditions, and correlations between the center of field and a second point farther out in the mixing layer would be weaker. Second, consider the direction of the line S. Downstream of the fixed reference point, the line is clearly heading in a negative ξ_3 (i.e., $-z$) direction. Upstream, there is some arbitrariness involved, but the line also has a negative ξ_3 heading. From the flow pattern the impression is that the flap is again quite effective in turning the flow. At a positive delay time, the particles that were at the reference point have moved steadily downward toward the surface of the flap, and thus a stronger correlation level exists. The same type of agreement can also be made for the flow upstream of the reference point.

IV. Summary

Auto- and cross-correlations were determined for the concentration field at various downstream locations. At $x/2r_0 = 4$, the autocorrelation coefficient curve was found to possess a damped sinusoidal nature for the three different flow configurations. The concentration fluctuations at $y = \pm 0.5$ were found to be related both at $x/2r_0 = 4$ and $x/2r_0 = 8$. The maximum absolute values of the cross correlation coefficient did, however, decrease sizably from four to eight diameters downstream of the exit plane. The power spectra for the jet, jet/plate, and jet/flap all exhibited a peak at $x/2r_0 = 4$ at approximately the same frequency as that found in the core velocity spectra. Here again, evidence exists in reinforcement of the vortex model of the jet. The plate and flap did seem to diminish the peak and also seemed to cause a shift of energy to lower frequencies in the spectra.

Space-time correlations for the turbulent velocity fields were obtained, and the lines of maximum maximorum were constructed for both the x-z plane and y-z plane. For the unconfined jet, the isocorrelation levels were symmetric with respect to the ξ_1 axis though very elongated. The line of maximum maximorum was straight and parallel to the ξ_1 axis. In the y-z plane, the isocorrelation levels were circular in shape about the ξ_1 axis. For the flow over the plate, the isocorrelation curves in the x-z plane were very complicated and elongated in the ξ_1 direction, and the line of maximum maximorum was curved convex toward the wall both upstream and downstream of the fixed reference "probe." For the flow over the flap, the isocorrelation curves were elongated and rotated down toward the surface in the x-z plane; evidence also existed as to confirm the effectiveness of the flap in turning the flow. The isocorrelation contours for the turbulent flowfields demonstrate the existence of large-scale structures. Consider the fact that the shape of the contours is significantly different for each of the three flow configurations in both the x-z and y-z planes. The flow knows whether or not a confining surface is present and also senses if the wall is curved or flat. This knowledge is then seemingly transmitted throughout the flowfield.

Acknowledgment

This work was supported in part by NSF Grant ENG75-22488 and NASA Grant NGR47-005-219.

References

[1] Catalano, G. D., Morton, J. B., and Humphris, R. R., "An Experimental Investigation of an Axisymmetric Jet in a Coflowing Airstream," *AIAA Journal*, Vol. 14, Sept. 1976, pp. 1157-1158.

[2] Catalano, G. D., Morton, J. B., and Humphris, R. R., "An Experimental Investigation of a Three-Dimensional Wall Jet," *AIAA Journal*, Vol. 15, Aug. 1977, pp. 1146-1152.

[3] Ko, N. W. M. and Davies, P. O. A. L., "The Near Field Within the Potential Core of Subsonic Cold Jets," *Journal of Fluid Mechanics*, Vol. 50, Pt. 1, Nov. 1971, pp. 49-78.

[4] Bradshaw, P., Fevis, D. H., and Johnson, R. J., "Turbulence in the Noise Producing Region of Circular Jets," *Journal of Fluid Mechanics*, Vol. 19, Pt. 4, Aug. 1964, pp. 591-624.

[5] Kline, S. J. and Runstalder, P. W., "Some Preliminary Results of Visual Studies of the Flow Model of the Wall Layer of the Turbulent Boundary Layer," *Journal of Applied Mechanics*, Vol. 26E, No. 166, June 1959.

[6] Brown, G. L. and Roshko, A., "On Density Effects and Large Scale Structure in Turbulent Mixing Layer," *Journal of Fluid Mechanics*, Vol. 64, Pt. 4, July 1974, pp. 775-816.

[7] Davies, P. O. A. L., "Turbulence Structure in Free Shear Flows," *AIAA Journal*, Vol. 4, Nov. 1966, pp. 1971-1978.

[8] Crow, S. C. and Champagne, F. H., "Orderly Structure in Jet Turbulence," *Journal of Fluid Mechanics*, Vol. 48, Pt. 3, Aug. 1971, pp. 547-591.

[9] Yule, A. J., Bruun, H. H., Baxter, D.R.J., and Davies, P.O.A.L., "Structure of Turbulent Jets," University of Southampton, ISVR Memo No. 506, 1965.

[10] Favre, A. J., Gaviglio, J. J., and Dumas, R., "Space-Time Double Correlations and Spectra in a Turbulent Boundary Layer," *Journal of Fluid Mechanics*, Vol. 2, Pt. 4, April 1957, pp. 313-342.

[11] Favre, A., "Review on Space Time Correlations in Turbulent Fluids," *Journal of Applied Mechanics, Transactions of ASME*, Vol. 32 F, No. 241, 1965.

[12] Sternburg, J., "On the Interpretation of Space Time Correlation Measurements in Shear Flow," *The Physics of Fluids*, Supl. 10, Pt. 11, S 146, 1967.

[13] Fisher, M. J. and Davies, P.O.A.L., "Correlation Measurements in a Non-Frozen Pattern of Turbulence," *Journal of Fluid Mechanics*, Vol. 18, Jan. 1964, pp. 99-116.

[14] Favre, A. J., Gaviglio, J., and Fohr, J. P., "Spectral Distributions in a Turbulent Boundary Layer," Office National d'Etudes et de Recherches Aerospatiales, TP No. 164, 1964.

[15] Schoenster, J. A., Willis, C. M., Schroeder, J. C., and Mixson, J. S., "Acoustic Loads Research for Powered Lift Configurations," Powered-Lift Aerodynamics and Acoustic Conference, Langley Research Center, Hampton, Va., May 1976.

[16] Shaughnessy, E. J. and Morton, J. B., "Measurements of Particle Diffusion in a Turbulent Jet by Laser Light Scattering," *Journal of Fluid Mechanics*, Vol. 80, Pt. 1, April 1977, pp. 129-148.